

Measurement of dynamic strain using an optic fibre system in adaptive composite laminates with an integrated piezoelectric sensor/actuator

CARLOS A. RAMOS¹, RUI DE OLIVEIRA², ANTÓNIO T. MARQUES³, ORLANDO FRAZÃO^{4*}

¹Instituto Superior de Engenharia do Porto (ISEP),
Rua Dr. António Bernardino de Almeida 431, 4200-072, Porto, Portugal

²Instituto de Engenharia Mecânica e Gestão Industrial (INEGI),
Rua Dr. Roberto Frias, 400 4200-465 Porto, Portugal

³Departamento de Engenharia Mecânica e Gestão Industrial (DEMEGI),
Faculdade de Engenharia da Universidade do Porto (FEUP),
Rua Dr. Roberto Frias, s/n 4200-465 Porto, Portugal

⁴Instituto de Engenharia Electrónicos e Sistemas de Computadores (INESC Porto),
Rua do Campo Alegre 687, 4169-007 Porto, Portugal

*Corresponding author: ofrazao@inescporto.pt

This study seeks the development of adaptive composites capable to monitor and actively damp vibrations. In the proposed material, vibrations measurements are performed by an embedded low finesse optical fibre extrinsic Fabry–Pérot interferometer, while active damping will be performed by embedded piezoelectric ceramics. This paper focuses on the development of the monitoring procedure. The proposed interrogation procedure for the low finesse optical fibre extrinsic Fabry–Pérot interferometer was successfully used to monitor the composite plate when submitted to four-point bending dynamic tests at different frequencies. The embedding of both sensing and actuating components in carbon-fibre reinforced composite laminates is also presented. In the case of the actuator, the efficiency of the embedding process was merely analysed from the capability of the piezoelectric ceramic to monitor dynamic strain of the composite using the PZT piezoelectric inverse effect.

Keywords: smart composite materials, health monitoring, Fabry–Pérot interferometer, piezoelectric ceramic.

1. Introduction

Smart composite materials with different embedded sensors have been lately subject of a particular attention in fields beyond the so-called traditional engineering. The embedding of sensors in the material at its manufacturing is one of the challenges

to which material science is confronted. It is thus necessary to overcome some of the existing barriers, namely to what concerns the knowledge of those sensors, after their embedment, and when submitted to predetermined actions.

Optical fibre and piezoelectric effect-based sensors are among the existing sensors the most commonly used for smart composite material applications. The first ones have the advantage to be less intrusive when embedded due to their low dimension. These sensors can be used for health monitoring of composite materials from, for example, strain and acoustic emission measurement [1]. The brittleness of the ingress/egress point in the composite structure can be a weakness for its application in industrial environment. In the case of piezoelectric sensors this point is not problematic. However, due to its higher dimensions, the embedding of the piezoelectric element is more complex, in particular, in carbon fibre reinforced composite material due to the carbon electrical conductivity.

The high strain sensitivity of piezoelectric sensors combined to their fast response makes of this sensing device a good candidate for health monitoring of smart composite material. *In situ* active damage detection procedures, in particular at impact, have been implemented, for composite structures, based on vibration [2] and Lamb waves [3, 4] sensing using embedded sensors. Recent advances in the use of printed circuit board techniques make it possible to embed piezoceramics with minimal impact on the original system [4, 5].

In this study, a hybrid system is proposed for vibration monitoring and control. A low finesse optical fibre extrinsic Fabry–Pérot interferometer (EFPI) sensor is used for vibration measurements high resolution [6, 7], whereas a lead zirconate titanate piezoceramic (PZT), with a thickness of 0.3 mm, is used for its actuation properties. The embedding process of sensor and actuator, in carbon-fibre/epoxy laminates is implemented. The embedment effectiveness for both elements is verified from their capacity to efficiently sense dynamic strains in the composite after embedding.

2. Sensor/actuator embedding

2.1. Extrinsic Fabry–Pérot interferometer sensor

A low finesse EFPI (Fig. 1) based on the interference of two electromagnetic waves was used in this study. It consists of two parallel plans separated by a distance L .

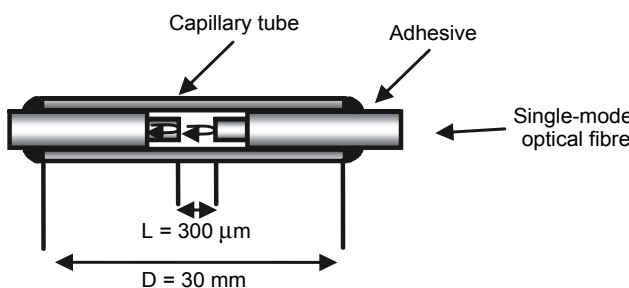


Fig. 1. Low finesse optical fibre EFPI sensor.

The parallel mirrors are aligned with their normal in the direction of propagation of a plane lightwave. The reflective plans consist of single-mode optic fibres ends cut at 90° providing a reflection of Fresnel of 4% of the light at the air/silica interface. The alignment of the optic fibres was guaranteed by a silica capillary tube with an outer diameter slightly superior to the optic fibre around 250 µm.

In the case of a low-finesse EFPI, the output signal is a quasi-sinusoidal. The interference pattern observed when illuminating the EFPI sensor by a broadband light is presented in Fig. 2. The EFPI does not provide a direct value of the wave displacement. To obtain definitive results it is necessary to proceed to a demodulation. A deformation of the host material will produce small phase shifts. When measuring small phase shifts, it is desirable to operate along the linear region of the response curve (Fig. 3), *i.e.*, the region between the peaks and valleys, as it gives the largest change in reflected intensity for a given phase shift of light. At quadrature, the relation between phase shift and reflected intensity is linear.

It is essential to maintain the quadrature point of operation for maximum sensitivity. Numerous techniques have been developed to stabilize interferometric systems [8–10], *e.g.*, the use of frequency and phase modulators for active stabilization by tuning the frequency of the laser source, or phase compensation using piezoelectric elements.

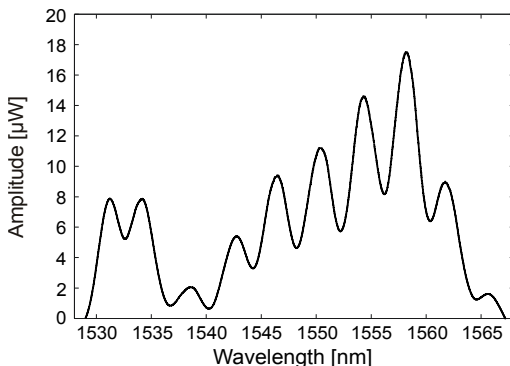


Fig. 2. Spectral response of the EFPI.

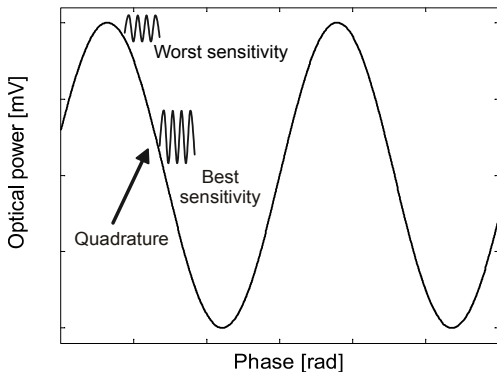


Fig. 3. Transfer function curve of the EFPI.

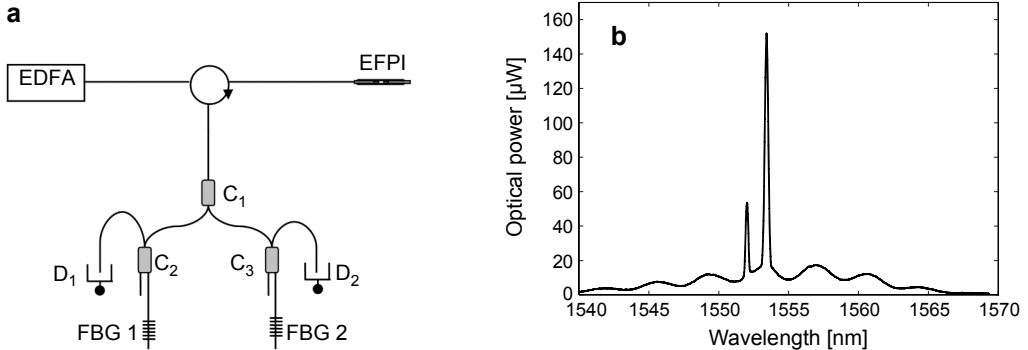


Fig. 4. Experimental set-up for the EFPI interrogation (a) and wavelength spectrum and the reflected light by the two FBG (b).

Using two phase signals out of phase by 90° , it is possible to stabilize the interferometer readout sensitivity. The ability of the fibre Bragg grating (FBG) to select a spectral bandwidth, when illuminated by a broadband optical source (EDFA), was used for phase recovery. It was thus possible to obtain, from two wavelengths, two signals with their phase in quadrature. The experimental set-up is represented in the Fig. 4a. In Figure 4b is represented the optical power spectrum measured by an optical spectrum analyzer measured at C_1 when allowing the light to be reflected at extremities of the two FBG. The light reflected by the two FBG (*i.e.*, the intensity of the two peaks in the Fig. 4b) is converted to electrical signals through photodetectors from JDS Uniphase with bandwidth of 100 kHz (D_1 and D_2).

The two FBG reflect a narrow band of the light. These bands are centred on a wavelength, *i.e.*, the Bragg wavelength (Eq. (1)). The Bragg wavelengths are chosen in such a way to have the two signals in quadrature of phase and in such a way to operate along the linear region of the response curve. The phase δ is obtained from the equation [11]

$$\delta = \tan^{-1} \left(\frac{v_2 - V_2}{v_1 - V_1} \right) \quad (1)$$

where $V_{1,2}$ are constant voltages dependent on the optical power and the gain in the detection electronics and v_1 and v_2 the output voltages of the two photodetectors. The phase is correlated to the length cavity. The cavity length L of the EFPI can be measured from the modulation in the reflected spectrum by counting the number of fringes over a specified wavelength range from λ_3 to λ_4 . The relation between the cavity length and the wavelengths is then given as follows [12]

$$L = \frac{m\lambda_3\lambda_4}{2(\lambda_4 - \lambda_3)} \quad (2)$$

where the phase difference at wavelength λ_3 and λ_4 is $2m\pi$ and m an integer. Thus the strain of the sensor can be calculated according to the following equation

$$\varepsilon = \frac{\Delta L}{D} \quad (3)$$

Such procedure is applicable for static strain measurements, but is not appropriate for the case of vibrations because the method requires the use of the optical spectrum analyzer which is too slow. For dynamic strain, the cavity length L is obtained from the phase variation $\Delta\delta$ as follows

$$L = \frac{\Delta\delta}{4\pi\left(\frac{1}{\lambda_1} - \frac{1}{\lambda_2}\right)} \quad (4)$$

λ_1 and λ_2 were chosen in such a way that $\Delta\delta = \pi/2$.

2.2. Piezoelectric ceramic

The chosen actuator was a PX5-N (Morgan Electronics) piezoelectric ceramic with $12 \times 12 \times 0.3$ mm³ and polarized perpendicularly to electrode planes. The PZT characteristics are listed in Tab. 1. The PZT actuator was embedded in a preliminary study in-between two layers of CFRP CC206 twill 2/2 from Seal in a preliminary study whose finality was to develop the embedment procedure [13].

Table 1. Material properties of the PZT.

Parameters	
Density	7.80 g/cm ³
Poisson's ratio	0.31
Charge constant d_{31}	-195×10^{-12} m/V
Charge constant d_{33}	450×10^{-12} m/V
Voltage constant g_{31}	25×10^{-3} m/V
Voltage constant g_{33}	-11.5×10^{-3} m/V
Elastic constant E_{11}	22.5 GPa
Curie temperature	350 °C

The PZT ceramic was embedded in the middle layers. High-temperature wires were soldered to the ceramic, insulated from the carbon substructure by high-temperature materials. After lay-up, the CFRP laminate was vacuum-bagged and placed in an autoclave. The curing cycle was constituted by a heating ramp of 4 °C/min, a plateau of one hour at 125 °C, which is significantly lower than PZT Curie temperature, followed by cooling-down at 1.5 °C/min. A pressure of 0.1 N/mm² was applied as well as an internal vacuum of 0.085 N/mm². To embed a PZT element into CFRP

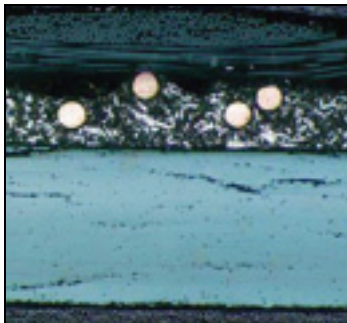


Fig. 5. Microscopy observation of the embedded PZT.

composites, some issues have to be dealt with, in particular, electrical insulation. Embedded sensors can become short-circuited during the autoclave stage. Insulating films were used to prevent the anode and cathode of the PZT coming into contact with carbon fibres during curing. A plate having a nominal thickness of 0.4 mm was obtained. High-temperature wires were soldered to the ceramic, insulated from the carbon substructure by high-temperature materials. An insulating film was used to prevent the anode and cathode of the PZT from coming into contact with carbon fibres during curing (*cf.* microscopy image in Fig. 5).

The integrity of the PZT element was qualitatively verified after embedding from resistance measurements. The capacity of the PZT element to generate and transmit vibration in the composite material was quantitatively verified through electronic speckle pattern interferometry (ESPI) observations [14]. Voltages ranging from 5 V to 100 V were applied. The specimen was rigidly fixed in one end, thus the actuator displacement induced a flexural displacement in the rigid body. The maximum variation of the laminate plate's profile was taken as the displacement induced by the actuator. A linear relationship was observed between the actuation displacement and the input voltage for that low applied voltage. The factor between the surface displacement and the applied voltage is 0.064 $\mu\text{m}/\text{V}$ for that specific thin plate.

2.3. The smart composite structure

In this study, thicker composite plates, with nominal dimensions of $200 \times 50 \times 1 \text{ mm}^3$, were produced in an autoclave, using two layers of woven carbon/epoxy preprints (CC206 twill 2/2 from Seal) and four intermediary layers of unidirectional carbon/epoxy preprints (HS160-REM from Seal). Lamina mechanical properties are summarized in Tab. 2. The PZT was embedded in the mid-layer of the composite (Fig. 6a). The EFPI sensor was inserted in the same layer at a distance of 130 mm.

Table 2. Lamina mechanical properties.

Material	E_1 [GPa]	E_2 [GPa]	v_{12}	G_{12} [GPa]
Twill	57	57	0.024	2.29
Unidirectional	131.6	8.7	0.33	3.5

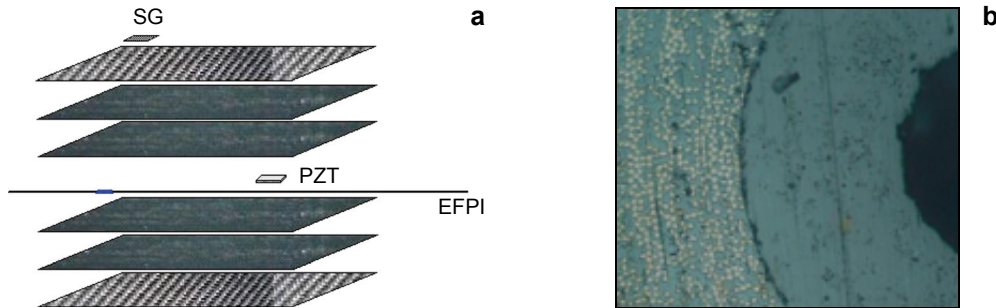


Fig. 6. Composite lay-up (a) and microscopy observation (b) of EFPI embedment.

The good embedding of the EFPI sensor was observed by microscopy image (Fig. 6b). It was also observed that the sensor and actuator are not at the neutral line of the plate.

3. Dynamic strain measurements

Dynamic tests were performed to verify the effectiveness of the optical fibre system for vibration measurements. The composite plate was loaded in four-points bending under dynamic solicitation. Loading was applied at a frequency varying from 10 to 100 Hz with steps of 30 Hz. The maximum frequency was imposed by the limit of the mechanical testing apparatus. The maximum displacement length was at the centre of specimen length of 2 mm.

The integrity of sensing and actuating elements, after their integration, as well as the quality of their embedment in the composite were verified from their sensing capability of dynamic strain [15, 16]. An electrical strain gage was glued at the plate surface to verify the reliability of EFPI and PZT responses. The response of the PZT, the electrical strain gage and the EFPI were simultaneously recorded in a Spider 8 acquisition system from HBM. Data were acquired at 1 kHz. The signals of the PZT and EFPI are given in volts. The PZT element factor, *i.e.*, the strain to voltage relationship is different after embedding, depending on the host material, and can be

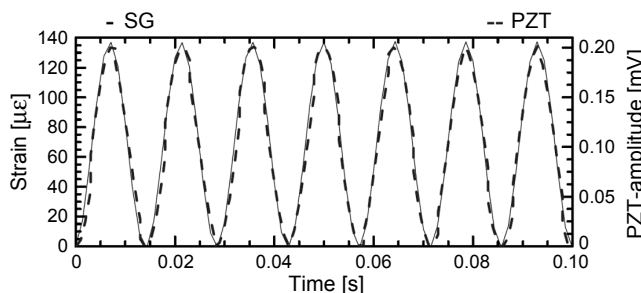


Fig. 7. Relationship between the PZT response and the composite longitudinal strain at 70 Hz.

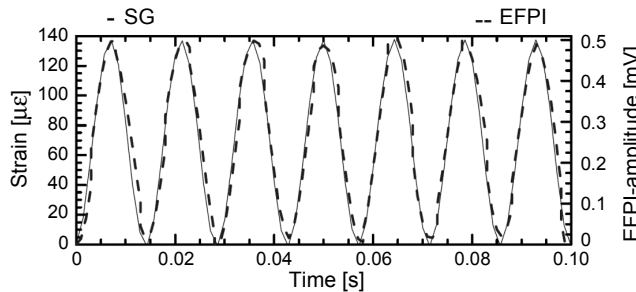


Fig. 8. Relationship between the EFPI response and the composite longitudinal strain at 70 Hz.

measured by ESPI as already mentioned. The relationship between the recorded signal, in volts, and the strain for the EFPI can be obtained using Eqs. (1), (3) and (4). In Figures 7 and 8 are presented the time responses during *ca.* 0.14 s of the PZT element and of the EFPI sensor for a solicitation at a frequency of 70 Hz.

The PZT and EFPI provided similar reliability to this frequency. The amplitude of the response for the two devices was constant for frequencies up to 100 Hz (Fig. 9). This permits to conclude that both sensing and actuating elements were successfully embedded in the composite. The proposed optical fibre system successfully measured dynamic strain. In a previous study [13], another optical fibre sensor, *i.e.*, fibre Bragg grating (FBG), was considered for that purpose. An FBG was embedded in a composite plate with the same dimensions that was also tested under the same conditions. A commercially available high-speed FBG interrogator from fibre sensing (SA), a BraggSCOPE, based on a broadband optical source and optical filtering technology was used. The use of FBG for the dynamic strain measurement at such frequencies was not convincing. For such application, strain values measured by the FBG sensor should be provided through the conversion of optical power variations into wavelength shifts [17]. When comparing the two optical fibre sensor systems, the combination of the proposed interrogation procedure for low-finesse EFPI sensor appears to be more reliable for high frequency strain measurements than FBG sensors interrogated by the BraggSCOPE.

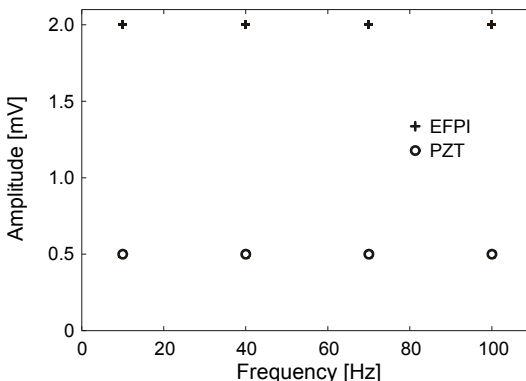


Fig. 9. Variation of the amplitude of sensors response vs. solicitation frequency.

4. Conclusions

Advanced composites with an optical fibre low-finesse EFPI sensor and a PZT sensor/actuator were successfully implemented. The proposed embedding methodology guarantees the integrity of sensing and actuation elements. An original sensing methodology based on a low-finesse EFPI, interrogated by the generation of two signals in quadrature of phase using two FBGs, was proposed and proved to be adequate for vibration monitoring. The embedment of PZT element is more complex and more intrusive than optical fibre sensors, in particular, due to the presence of the connecting wires and the carbon fibre electrical conductivity. PZT are therefore not the best solution for the development of build-in sensor networks in composites. Due to their actuation potential and applicability for energy harvesting, the combination of these elements with other sensors, such as optical fibre based, is promising.

Acknowledgements – The financial support of the Portuguese Foundation for Science and Technology (FCT) and European Social Fund (ESF) under project SMARTCOAT (PTDC/EME-PME/108308/2008) is gratefully acknowledged.

References

- [1] DE OLIVEIRA R., RAMOS C.A., MARQUES A.T., *Health monitoring of composite structures by embedded FBG and interferometric Fabry–Pérot sensors*, Computers and Structures **86**(3–5), 2008, pp. 340–346.
- [2] YAN Y.J., YAM L.H., *Online detection of crack damage in composite plates using embedded piezoelectric actuators/sensors and wavelet analysis*, Composite Structures **58**(1), 2002, pp. 29–38.
- [3] MONNIER T., *Lamb waves-based impact damage monitoring of a stiffened aircraft panel using piezoelectric transducers*, Journal of Intelligent Material Systems and Structures **17**(5), 2006, pp. 411–421.
- [4] YANG S.M., HUNG C.C., CHEN K.H., *Design and fabrication of a smart layer module in composite laminated structures*, Smart Materials and Structures **14**(2), 2005, pp. 315–320.
- [5] CHRISTMAS S.P., *High-resolution vibration measurements using wavelength-demultiplexed fiber-Fabry–Pérot sensors*, 14th International Conference on Optical Fibre Sensors, Conference, Vol. 4185, 2000 pp. 11–13.
- [6] ZHONGQING SU, XIAOMING WANG, ZHIPING CHEN, LIN YE, DONG WANG, *A built-in active sensor network for health monitoring of composite structures*, Smart Materials and Structures **15**(6), 2006, pp. 1939–1949.
- [7] CHANG Y.-H., KIM D.-H., HAN J.-H., LEE I., *Online phase tracking of interferometric optical fiber sensors for vibration control*, Journal of Intelligent Material Systems and Structures **18**(4), 2007, pp. 311–321.
- [8] MEASURES R., *Fiber optic strain sensing*, [In] *Smart Structures*, [Ed.] Udd E., John Wiley & Sons, New York, 1995.
- [9] KIM D.H., KOO B.Y., KIM C.G., HONG C.S., *Damage detection of composite structures using a stabilized extrinsic Fabry–Pérot interferometric sensor system*, Smart Materials and Structures **13**(3), 2004, pp. 593–598.
- [10] READ I., FOOTE P., MURRAY S., *Optical fibre acoustic emission sensor for damage detection in carbon fibre composite structures*, Measurement Science and Technology **13**(1), 2002, pp. N5–N9.

- [11] DE OLIVEIRA R., FRAZÃO O., SANTOS J.L., MARQUES A.T., *Optic fibre sensor for real-time damage detection in smart composite*, Computers and Structures **82**(17–19), 2004, pp. 1315–1321.
- [12] LIU T., WU M., RAO Y., JACKSON D.A., FERNANDO G.F., *A multiplexed optical fibre-based extrinsic Fabry–Perot sensor system for in-situ strain monitoring in composites*, Smart Materials and Stuctures **7**(4), 1998, pp. 550–556.
- [13] RAMOS C.A., DE OLIVEIRA R., MARQUES A.T., *Implementation and testing of smart composite laminates with embedded piezoelectric sensors/actuators*, Materials Science Forum **587–588**, 2008, pp. 645–649.
- [14] MARQUES M.A., MONTEIRO J., RAMOS C.A., VAZ M.A., MARQUES A.T., *Actuator capabilities of piezoelectric devices embedded in composite laminate*, Materials Science Forum **587–588**, 2008, pp. 237–240.
- [15] MALL S., *Integrity of graphite/epoxy laminate embedded with piezoelectric sensor/actuator under monotonic and fatigue loads*, Smart Materials and Stuctures **11**(4), 2002, pp. 527–533.
- [16] EDERY-AZULAY L., ABRAMOVICH H., *The integrity of piezo-composite beams under high cyclic electro-mechanical loads – experimental results*, Smart Materials and Stuctures **16**(4), 2007, pp. 1226–1238.
- [17] HONGO A., KOJIMA A., KOMATSUZAKI S., *Applications of fiber Bragg grating sensors and high-speed interrogation techniques*, Structural Control and Health Monitoring **12**(3–4), 2005, pp. 269–282.

*Received May 31, 2010
in revised form July 27, 2010*